

FLUID MECHANICS OF THE THALLUS OF AN INTERTIDAL RED ALGA, *HALOSACCION GLANDIFORME*

STEVEN VOGEL AND CATHERINE LOUDON

Department of Zoology, Duke University, Durham, North Carolina, 27706

ABSTRACT

The elongate, ellipsoidal thalli of *Halosaccion glandiforme* (Gmel.) Rupr. are alternately exposed and immersed with tidal cycles. These sea water-filled thalli are penetrated, mainly in the distal third, by 5 to 15 pores. During emersion, water is lost by evaporation from the surface of the thallus and by bulk flow through the pores; surface tension at the pores prevents entry of air. During reimmersion, thalli reinflate as a result of the elasticity of their walls and via pressure differences due to flow of ambient water along their surfaces. The drag of thalli is low, and, concomitantly, separation of flow is well downstream; as a result, their relatively weak stipes are adequate to resist hydrodynamic forces.

INTRODUCTION

Halosaccion glandiforme (Gmel.) Rupr. is a common inhabitant of relatively sheltered rocky coastal areas of the north Pacific. Its thallus forms a nearly symmetrical fusiform body of revolution up to 25–30 cm long, 3–4 cm in diameter, distally rounded, and tapering proximally to a thin, short stipe. The thallus is thin-walled (about 200 μm), filled with sea water (and usually about a cubic centimeter of gas), and punctured by 5 to 15 irregularly shaped (often cruciform) pores up to 200 μm across. A gentle squeeze squirts tiny streams of water from the larger pores. On San Juan Island, Washington, the algae occur mainly in the lower intertidal zone; a receding tide exposes water-filled thalli which then gradually lose varying amounts of water. This loss of water typically results in lateral and then bilateral compression of the thalli without entry of air. Upon reimmersion, the algae reinflate. Just before and immediately after exposure, the algae are subjected to the relatively rapid currents generated as surface waves interact with rocks.

The shape of the thallus suggests some degree of streamlining, an unusual occurrence in a sessile organism exposed to currents which are far from unidirectional. For streamlining to be functional, *Halosaccion* must operate as a weathervane, a behavior more common among planar, flexible forms (Vogel, 1984).

The water within the thallus appears to reduce desiccation or heating of tissue during periods of emersion. Thus DePamphilis (1978) found that three hours of exposure on a sunny summer day killed plants whose internal water had been removed but did not kill intact plants. And Muenschler (1915) noted that the length of exposure needed to dry the algae beyond the point of recovery increased with the amount of water inside the thallus.

The torpedo-like shape and perforation of a sea water-filled thallus and its cyclic deflation and inflation are unique among marine algae (Hansen, pers. commun.). The present study is an inquiry into the identity and relative contribution of the

various physical processes which might be concomitant with this peculiar morphology and behavior. Our focus is on devices which (1) determine the rate of water loss and prevent entry of air when the thallus is emersed, (2) enable replacement of water after reimmersion, and (3) prevent dislodgement of an alga by hydrodynamic forces.

Several agencies might, *a priori*, be involved. (1) Since a water-filled bag is exposed to air, *surface tension* must be considered, either of a cylindrical film of water around the thallus or of spherical interfaces at the pores. (2) Since evaporation occurs on the outside only, *concentration gradients* will develop. (3) Since a thallus has a preferred "resting" shape, inflated rather than flat, *elasticity of the thallus wall* is appreciable. (4) Since water can clearly flow through the pores, the *resistance of the pores to bulk flow* may be important in determining rates of water movement. Since environmental water currents may be substantial, (5) *drag*, (6) the *mechanical strength of the stipe*, and (7) *pressures generated by flow around the thallus* deserve attention. In some concerted fashion, these factors must accomplish the three functions mentioned above.

Clearly, the distribution and abundance in nature of an organism such as *Halosaccion* must be profoundly influenced by its adaptations to the physical conditions of the environment. The present study attempts to elucidate major components of that adaptation. It does not involve direct measurement of the relevant environmental variables nor does it address the precise habits of the organism in nature. These crucial matters are currently the subject of another investigation (Ladd Johnson, pers. comm.).

MATERIALS AND METHODS

Formulas and conventions

The following formulas will be employed in this paper.

(1) The Reynolds number, a dimensionless index to the character of flow (Vogel, 1981):

$$\text{Re} = \frac{\rho l U}{\mu} \quad (1)$$

(where μ is the dynamic viscosity of the medium, l a characteristic length of the immersed object, U the relative velocity of fluid with respect to object, and ρ the density of the medium).

(2) The drag coefficient, a dimensionless drag (Vogel, 1981):

$$C_d = \frac{2D}{\rho S U^2} \quad (2)$$

(where D is the drag and S is a specified area characterizing the object).

(3) Flow through a circular aperture (Happel and Brenner, 1965):

$$Q = \frac{a^3 \Delta P}{3\mu} \quad (3)$$

[where Q is total flow (volume per time), a the radius of the aperture, and ΔP the pressure difference across the aperture]. For sharp-edged apertures of no depth, the equation is trustworthy up to a Reynolds number of 3.2 based on pore diameter and mean velocity through the pore. For pores which are neither sharp-edged, negligibly deep, nor circular in cross-section, this equation is not strictly applicable, but it can be used to calculate (from pressure and flow measurements) "nominal diameters"

for the pores—the diameters of functionally equivalent circular pores of negligible depth.

(4) Pressure difference across (a) spherically or (b) cylindrically curved air-water interfaces (Rouse, 1946):

$$\Delta P = \frac{2\gamma}{a} \quad (4a)$$

$$\Delta P = \frac{\gamma}{a} \quad (4b)$$

(where γ is surface tension and a here is the radius of curvature of the interface). If a is approximated by the radius of a pore and if wetting of the thallus is incomplete, then (4a) will overstate the pressure difference necessary to force air through a pore into a water-filled thallus.

(5) Resistance to flow through an aperture or pipe:

$$R = \frac{\Delta P}{Q} \quad (5)$$

The ratio of pressure difference to total flow is obtained from either (3) above or the Hagen-Poiseuille equation; for laminar flow, resistance is independent of speed.

(6) Pressure coefficient (Goldstein, 1938):

$$C_p = \frac{2\Delta P}{\rho U^2} \quad (6)$$

Pressure coefficient is analogous to drag coefficient (and, like the latter, is dimensionless). When shifting media to facilitate the use of models, maintaining constancy of the Reynolds number assures constancy of pressure coefficient, not pressure; and the latter must be recomputed with this formula.

The following values of physical parameters have been used: (1) surface tension of sea water, 0.074 N m^{-1} ; (2) density of sea water, $1.03 \times 10^3 \text{ kg} \cdot \text{m}^{-3}$; (3) viscosity of sea water, $1.36 \times 10^{-3} \text{ kg} \cdot \text{m}^{-1} \cdot \text{s}^{-1}$; all for 12°C ; (4) density of air, $1.18 \text{ kg} \cdot \text{m}^{-3}$; (5) viscosity of air, $18.3 \times 10^{-6} \text{ kg} \cdot \text{m}^{-1} \cdot \text{s}^{-1}$; the latter at 25°C .

As used here, "imprecision" refers to the standard deviation of a series of measurements whether calculated or estimated without reference to any accepted value; "systematic error" is the maximum difference from some "true" value as a result of calibration artifacts; "uncertainty" combines the two either where systematic error is negligible compared to imprecision or where a distinction is impractical.

Equations (7) through (9) presume S.I. units.

Material

Specimens of *Halosaccion* ranging in length from 6 to 12 cm were collected from the northern shore of Friday Harbor ("Cantilever Point," Friday Harbor Laboratories) and the southern shore of the entrance to False Bay ("Mar Vista Resort"), both on San Juan Island, Washington, during August of 1981 and 1983. Collection typically involved gently pulling on and breaking the stipe; plants were maintained without attachment in running sea water at about 12°C at the Friday Harbor Laboratories and, except as noted, were used for experimental purposes within a day following collection. Additional algae were preserved in a solution of formalin in sea water buffered with sodium tetraborate for observations on the distribution of pores.

A brass model of a thallus (Fig. 1A) was constructed on a lathe in order to investigate the relationship between pressure and location on the thallus; the model was life-sized and differed from a normal alga only in being a fully symmetrical body of revolution. Measurements for the model were obtained from a projected lateral photograph of a small but otherwise ordinary specimen tethered by its cut stipe in a flow tank at $0.33 \text{ m} \cdot \text{s}^{-1}$; the "fineness ratio" (length divided by diameter) of the specimen was 3.55. Uncertainty in the dimensions of the model is estimated as 0.2 mm. A small hole penetrated the model axially from the apex almost to the stipe; at the apex this hole was continuous with a brass tube, 2.4 mm in diameter, which functioned as the support ("sting") and pressure-transmitting conduit. A lengthwise row of 15 additional holes of 1.0 mm diameter, each connecting the model's surface with the axial hole, served as pressure taps; in practice all but one of these latter holes were occluded by small pieces of plastic adhesive tape.

Pressure and total flow through the pores

For manipulations involving pressures in water above 200 Pa (N m^{-2}) the pressure chamber shown in Figure 1B sufficed; it consisted of two plexiglas plates, each with a 25 mm central hole, between which a piece of thallus sandwiched between rubber gaskets could be fit. Each hole communicated with a chamber and the latter with a fitting for the attachment of rubber tubing. Glass plates on the chambers permitted viewing the thallus as pressure changed. Pressures were applied by adjusting the

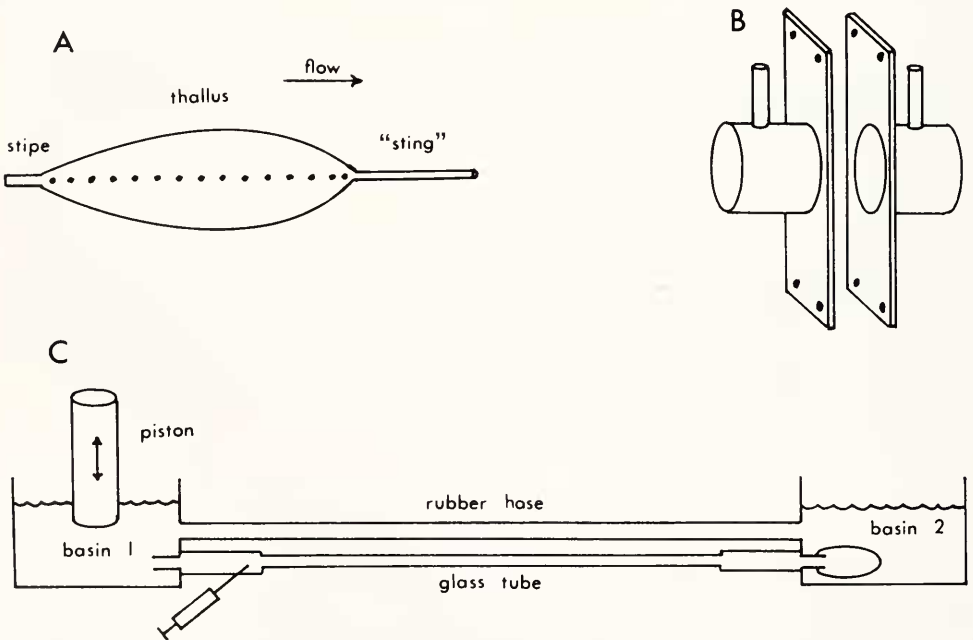


FIGURE 1. (A) Brass model of a *Halosaccion*, showing location of pressure taps; together, thallus and stipe are 62 mm in length. (B) Pressure chamber for use with pieces of thallus wall; rubber gaskets normally seal the piece of thallus between the halves of the chamber. (C) Apparatus for applying pressure to a cannulated thallus or for observing refilling due to wall resiliency. The glass tube attaches to the basins via short pieces of rubber tubing through which dye can be injected; both conduits connecting the basins are equipped with pinch clamps.

relative heights of the water columns on each side of the chamber. Uncertainty in the production of pressure differences was estimated as 10 Pa.

Where pressures in water were below 200 Pa, the apparatus of Figure 1C was used. Two rectangular basins were connected by a straight glass tube and appropriate fittings and by a rubber hose; either connection could be closed. Lowering a cylindrical piston into one basin using a precision worm-drive ("Unislide") raised its water level by a small amount since the piston area (62.1 cm^2) was much less than that of the air-water interface in the basin (403.3 cm^2). This interface was large enough to minimize the effects of surface tension. Uncertainty in the resulting pressure differences between the basins was estimated as 0.2 Pa. An entire thallus could be attached to an extension of the glass connection between the basins as shown in Figure 1C: a tapered plastic hose connector was inserted into the hole left after amputation of the stipe, and an annulus of latex tubing was rolled over the cut end of the thallus. Leakage was checked by injecting a sea water solution of fluorescein (uranine) into the nearest rubber tube and applying pressure.

With either pressure-producing apparatus, total flow was measured by injecting a pulse of fluorescein solution and timing the passage of the dye front through a glass tube, taking advantage of the consistent two-fold difference between axial flow speed and average speed for fully developed laminar flow. Minimum detectable total flow was $5 \text{ mm}^3 \cdot \text{s}^{-1}$; uncertainty was estimated as the larger of $5 \text{ mm}^3 \cdot \text{s}^{-1}$ or 3% of any determination.

Pressures in air were measured with a multiplier manometer constructed and calibrated as previously described (Vogel, 1981; 1983); imprecision was estimated as 0.1 Pa and systematic error as 0.2 Pa. A reference pressure was provided by a hole of 1.6 mm diameter flush with the surface and 28 mm downstream from the leading edge of a thin, flat plate parallel to the airflow.

External flows and force measurements

Measurements of drag and visualization of flow were done in a small flow tank with a working section 10 cm deep and 10 cm wide: the tank was designed as described previously (Vogel, 1981) except for two features. (1) A standpipe downstream from the working section and a tap in the return pipe permitted continuous exchange of sea water. (2) The drive consisted of two sequential propellers separated by a 6 cm long, three-vaned stator: the latter supported the shaft bearings, increased the advance ratio to about 1.1, and improved maximum speed, smoothness of flow, and efficiency. Calibration was done by timing the flow of dye pulses over a 50 cm course (best at low speeds) and by determining the drag of a circular disk oriented normal to flow, 3.73 cm in diameter, of known and constant drag coefficient (most useful at high speeds). Systematic error and imprecision are each estimated as 3% for flows more than 2 cm from either walls or air-water interface. For visualization of flow patterns, fluorescein was injected through the drawn end of a polyethylene catheter tube (tip diameter about 0.1 mm) by a micrometer-equipped syringe.

To measure drag, thalli were attached by their stipes to the end of a cylindrical "sting," 1.83 mm in diameter, which extended vertically out of the flow tank. The sting in turn attached to the end of an aluminum beam, $60 \text{ mm} \times 12.7 \text{ mm} \times 1.27 \text{ mm}$, with foil strain gauges centered on each face. The gauges formed two arms of a DC Wheatstone bridge, the imbalance of which was amplified by an Intersil ICL7605CJN instrumentation amplifier in the manufacturer's recommended circuit. Calibration, with an uncertainty of 1%, was done using balance weights with the beam held horizontally. Measurements of the drag of the sting alone were subtracted

from the data; the former figures agreed closely with calculations from flow speed and accepted values of drag coefficient, and thus they provided a check on flow and force calibrations.

The force necessary to pull a thallus from its attachment in nature was determined by connecting a string between a small alligator clip and an Ametek force gauge (T500G-TC), grabbing a stipe with the clip, and noting the highest force as the thallus came loose. Uncertainty was about 5%.

Airflow was produced by a large wind tunnel described by Tucker and Parrott (1970), calibrated with a whirling vane (axial flow) anemometer with an estimated systematic error of less than 5% and an imprecision of less than 2%.

Other methods

Salinity was measured with an American Optical hand-held salinity refractometer.

The location of holes in preserved specimens was determined on castings. Deflated thalli were filled with plaster of Paris through a cut in the stipe end, and the plaster was allowed to set while thalli were hung in water. The thalli filled with plaster were dipped in a basic fuchsin solution for two minutes, and the thalli were then peeled off the casting; purple spots marked hole locations.

RESULTS

Resistance of pores to flow

For low pressures, volume flow through the pores proved to be directly proportional to pressure. Total flow was determined on a thallus for eight pressures from 19.6 to 114 Pa by forcing water out of a cannulated thallus with the apparatus of Figure 1C. No threshold pressure was necessary to produce a detectable flow, and the resistance (corrected for that of the glass dye-timing tube) averaged $3.07 \times 10^9 (\pm 0.38 \times 10^9)$ $\text{N} \cdot \text{s} \cdot \text{m}^{-5}$ (equation 5) with little if any systematic variation with changes in applied pressure (see below). Forcing dye through the thallus, an automatic consequence of the measurements, indicated nine open pores in the thallus, so the resistance was equivalent to that of nine identical pores of $2.76 \times 10^{10} \text{ N} \cdot \text{s} \cdot \text{m}^{-5}$ resistance and $103 \mu\text{m}$ nominal diameter (equation 3). Using this nominal diameter and the average flow through the pores, the Reynolds numbers (equation 1) range from 35 to 250, well above the value of 3.2 given as the maximum for confident use of equation (3). A regression of log-transformed data, though, gave a slope of 1.10 for total flow as a function of pressure, so the assumption of direct proportionality in the equation is not seriously violated (the lack of sharp edges on the pores probably postponed the onset of turbulence to higher Reynolds numbers than otherwise expected):

$$Q = (2.206 \times 10^{-10})\Delta P^{1.10}, \quad r = 0.989 \quad (7)$$

For higher pressures, volume flow was no longer directly proportional to pressure. Total flow was determined for pressures from 1.56×10^3 to 5.97×10^3 Pa with a piece of thallus containing a single pore using the apparatus of Figure 1B; three measurements were made at each of seven values of pressure. With water on both sides of the tissue, no differences were noted between flows either in or out of the thallus, and again no threshold value of pressure was necessary to produce a flow. The equation determined by linear regression of log-transformed data was:

$$Q = (1.322 \times 10^{-9})\Delta P^{0.631}, \quad r = 0.916 \quad (8)$$

Here the exponent (0.631) was closer to the value of 0.5 expected for Reynolds numbers above 30,000 (Happel and Brenner, 1965) than to that of unity expected below 3.2. Resistance was no longer "ohmic," and nominal diameter could not be calculated without knowing an empirical orifice coefficient. Using a pore diameter of 200 μm , the range of Reynolds numbers was 640 to 1480. These results indicate essentially ordinary behavior for the pores: bidirectionally equal resistances and the expected change in the character of flow between low and high Reynolds numbers.

With the apparatus of Figure 1B, it was possible to establish an air-water interface across a pore and then to force either air or water across the interface. With water passing through the pore, the relationship between pressure and flow did not significantly differ from the results cited above. No threshold pressure was noted, nor were there appreciable differences between flow in the two directions. It appears that the surfaces of the thallus are sufficiently hydrophilic that wetting is essentially complete and surface tension is of no consequence to the passage of water.

By contrast, air did not easily pass through a pore within which an air-water interface was located. By watching the side exposed to water, it was easy to determine threshold pressures at which air bubbles began to cross the piece of thallus. These pressures ranged from 990 to 17,900 Pa, an eighteen-fold variation. Curiously, the threshold pressures increased steadily after collection: the minimum average pressure (1125 ± 116 Pa) was obtained for a pore tested on the day of collection and the maximum ($17,200 \pm 581$ Pa) six days after collection. Pores apparently occlude unless thalli are subjected to the normal tidal cycles of exposure and immersion. There was no appreciable difference in the pressures necessary to force air through pores in the two directions.

Using equation (4) for a spherical interface, the minimum pressure of 990 Pa corresponds to a circular pore with a diameter of 300 μm . The same pressure corresponds to a hydrostatic head of 9.8 cm of sea water, about equal to the maximum pressure of water inside one of the present thalli hanging vertically in air. Thus as long as an air-water interface is present to block pores it is quite unlikely that air can be drawn into an intact thallus.

Emptying and refilling

Three turgid thalli with initial masses (including contained water) from 6.5 to 13.0 g were placed on a horizontal piece of transparent plexiglas and exposed to direct sunlight for two hours. Each lost water at a steady rate, averaging $0.17 \pm 0.035\%$ of its initial weight per minute, a 20.4% loss during the exposure. For these plants, the rate of water loss was more nearly proportional to surface area than to mass or volume. Two other thalli with 1 mm holes at their bases (damage not uncommon in nature) lost water at more rapid rates: 0.28 and 0.31% of initial weight per minute.

An additional thallus was similarly exposed to sunlight for four hours, and a small sample of its internal water was drawn each hour for determination of salinity. During exposure, salinity rose from 30.0 to 41.0‰ while the mass of internal water dropped from 24.1 to 17.5 g. The product of salinity and mass for the five determinations averaged 721.7 (± 4.7) (g‰), the constancy of these data indicating negligible salt loss during exposure. It appears that under these conditions water loss occurs entirely by evaporation of pure water.

Thalli held vertically in air by their stipes, however, lost water more rapidly, typically losing over half their water during a two-hour exposure. Sea water, in fact, dripped off the thalli. Loss rates were highly variable, though, even among undamaged

thalli. By equation (3) a water loss of 5 ml in two hours with a 400 Pa (4 cm) hydrostatic pressure head implies a single pore of 38 μm diameter or nine identical pores of 18 μm .

When immersed in water, deflated thalli inevitably refilled, although the rates of reflation were quite variable. Two sets of measurements were made. Five thalli had as much water as possible gently squeezed out through the pores, with an average weight reduction of 87%. In the first ten minutes of reimmersion they regained water at 3.4 (± 2.2)% of their fully inflated weight per minute. Eleven measurements on four other thalli with an average weight reduction of 35% gave refilling rates averaging 1.9 (± 0.9)% per minute.

Spontaneous refilling in still water requires that the pressure within a thallus be below ambient. This pressure difference was measured by cannulating thalli in the apparatus of Figure 1C and then determining the rates at which partially deflated specimens refilled through a fixed resistance with the same water level in the two basins. In practice, the glass dye-timing tube provided the resistance and was calibrated by production of known pressures (using the cylindrical piston) with no thallus attached. Rates of refilling during these measurements were sufficiently higher than those cited above that flow through the pores was negligible. Five measurements were made on each of four thalli; the average pressure difference was 53.6 (± 26.3) Pa. Variability occurred mainly among the different specimens rather than among measurements on individual thalli: standard deviations for the latter averaged only 14.2 Pa. The variation for individual thalli seemed to depend upon the location of the concavity caused by deflation; functional wall resilience is not constant for a thallus, even at a given degree of deflation.

A refilling rate of 2.5%/min driven by an inflation pressure (due to wall resilience) of 53.6 Pa corresponds, by equation (3) to a single pore of a nominal diameter of 146 μm or to nine 70 μm pores.

Ambient flow and drag

Small surface waves generate substantial currents within about half a meter of the shore or bottom; observations of the movement of dye pulses indicate that flow speeds may routinely reach $1 \text{ m} \cdot \text{s}^{-1}$. Shortly before emersion and immediately after reimmersion, *Halosaccion* will be exposed to these flows. Since these elongate thalli with flexible attachments operate as weathervanes, overall flow will never deviate very much from an axial direction from stipe to apex whatever the spatial and temporal complexity of local currents. Consequently it is appropriate to observe the results of ambient flows on either thalli or models oriented parallel to flow in a unidirectional flow tank.

The most immediate and obvious result of water motion on an attached organism is a force directed parallel to flow tending to dislodge it, its drag. For an object of non-negligible frontal area at moderate or high Reynolds numbers, high drag is associated with an anterior point of separation of flow and a wide wake; low drag reflects a delayed, posterior separation and a narrow wake. Dye was injected around and behind each of four thalli in the flow tank at four speeds from 0.12 to 0.33 $\text{m} \cdot \text{s}^{-1}$, and the algae were photographed in side view (Fig. 2). The "separation point" was taken as the distance along the axis of the thallus from the stipe to where flow separated from the surface divided by the total length of the thallus. It was always well downstream and did not shift appreciably with changes in speed (S.D. < 0.025 for each individual). The separation point did vary among individuals, from 0.795 to 0.914; and the rank order among the four individuals matched that of the "finesness

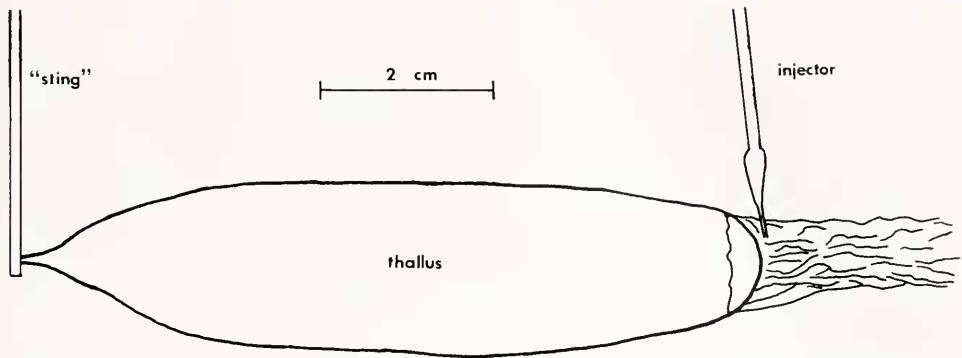


FIGURE 2. Tracing from a photograph taken during injection of dye into the wake of a thallus; dye moves upstream, "peels off" at the separation point, and marks the wake. The sting is idealized. Speed: $0.33 \text{ m} \cdot \text{s}^{-1}$; fineness ratio: 4.09.

ratio" (length over diameter), the latter ranging from 3.52 to 5.87. In short, separation occurred farther upstream in more rotund specimens.

A variety of measurements of drag were made on thalli of *Halosaccion*, of which the most complete set will be cited here; these were made on a particularly ordinary thallus and seem typical. The thallus had a length of 8.2 cm and a volume (calculated from its mass) of 8.85 cm^3 . Drag was measured at eleven speeds from 0.12 to $0.71 \text{ m} \cdot \text{s}^{-1}$, corresponding to Reynolds numbers (based on length) from 7450 to 44,100; data for drag were converted to drag coefficients (equation 2), with volume raised to the two-thirds power used as reference area. No discontinuities in the results were detectable; and, as will be discussed, the figures for drag were impressively low. The equation determined by the linear regression of log-transformed data for drag coefficient as a function of Reynolds number is

$$C_d = 608 \text{ Re}^{-0.86}, \quad r = 0.92 \quad (9)$$

How much force is, in fact, required to detach a thallus? Force to detach was measured for 20 thalli between 8.9 and 11.4 cm in length, all submerged while being pulled upon. Failure uniformly occurred at the stipe rather than the holdfast; $1.51 \pm 0.48 \text{ N}$ was required. Even the weakest attachment (0.88 N) had a strength about six times the weight of the thallus, so hanging during emersion puts an alga at no hazard of detachment. Nor is the drag measured at the highest speed of the flow tank near values needed for detachment: 0.0062 N at $0.71 \text{ m} \cdot \text{s}^{-1}$ is more than a hundred-fold too low.

Ambient flow and transmural pressures

In thalli, the concavities resulting from deflation first appear midway between base and apex. The pores, as determined by squeezing in air or, less violently, by observation of fuchsin spots on the castings, are predominantly located in the downstream third. If the pressure difference across the wall is more negative (net outward) near the middle than further downstream, a water current across a thallus could aid reinflation by causing a net inflow through the holes driven by this greater outward pressure on the middle of the thallus. It should be noted that both casual observations and measurements of elastic modulus (unpubl.) indicate that the thallus wall is functionally inextensible at the pressures of present interest.

Results of comparisons of refilling rates in still and in moving ($0.30 \text{ m} \cdot \text{s}^{-1}$) water were statistically equivocal: retrospectively, the speed chosen is likely to have been too low. Given the location of the investigators and the present interest in mechanisms as well as phenomena, recourse was made to the brass model described earlier.

The model was tested in the wind tunnel at speeds corresponding to water flows from 0.25 to $1.0 \text{ m} \cdot \text{s}^{-1}$. Converting data to pressure coefficients proved to reduce to insignificance variation resulting from the use of several speeds and thus allowed easy averaging of data. Inserting the density of water and the corresponding water velocities into equation (6) permitted calculation of the pressure differences which would obtain in the normal medium. Pooled and averaged data are shown in Figure 3; the graph is similar to one presented for streamlined bodies in Goldstein (1938—Fig. 215) which was obtained at Reynolds numbers nearly two orders of magnitude higher. Differences from published results on streamlined bodies are mainly in data from the downstream portion, near and behind the separation point, as expected for a body distally rounded rather than tapering to a point.

The strongly positive pressures near the upstream (stipe) end are probably of little functional significance since the upstream ends are stiffer, imperforate, and do not deflect observably inward in the flow tank. But the difference between the minimum pressure coefficient and that further downstream is of some interest. A difference of 0.063 corresponds to a pressure difference in sea water of 2.0 Pa at $0.25 \text{ m} \cdot \text{s}^{-1}$, 8.0 Pa at $0.50 \text{ m} \cdot \text{s}^{-1}$, and 32.0 Pa at $1.0 \text{ m} \cdot \text{s}^{-1}$. The latter figure, at least, is not insignificant when compared to the refilling pressure due to wall resiliency of around 50 Pa found earlier.

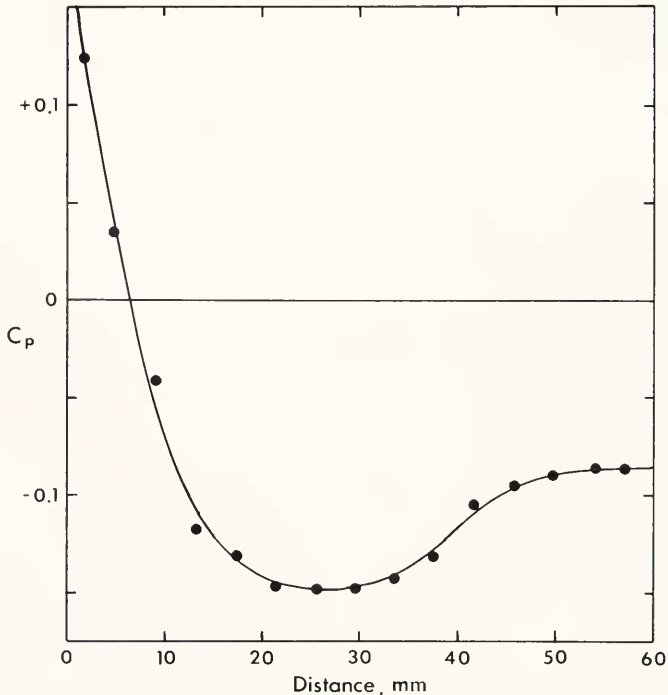


FIGURE 3. Pressure coefficient (equation 6) as a function of distance on the surface of the model thallus (Fig. 1A) from the stipe-thallus junction downstream to the apex, 60 mm in all.

DISCUSSION

Shape and drag

From several viewpoints, a thallus is well-designed to minimize drag. First, in absolute terms drag is low. At $0.65 \text{ m} \cdot \text{s}^{-1}$ ($\text{Re} = 40,700$ for the thallus) the drag of the thallus was 5.6 times lower than that of a sphere of the same frontal area (area projecting normal to flow) and 8.7 times lower than that of a sphere of the same overall volume. Indeed it is somewhat awkward to arrange a cylindrical “sting” for mounting a thallus which does not have more drag than the thallus itself. Concomitant with the low drag is the very rearward separation point—an object with a high drag coefficient such as a cylinder normal to flow or a sphere has a separation point at comparable Reynolds numbers about halfway from upstream to downstream extremity. In short, the thalli are impressively well streamlined. Streamlining, of course, works only for a narrow range of orientations of a body to the local flow; here it is facilitated by the flexible stipe and consequent automatic weathervaning.

Moreover, drag does not increase as drastically with increasing flow speed as it does for unstreamlined (bluff) bodies. In the present range of Reynolds numbers (of the order of 10^4), the drag of a bluff body is proportional to velocity to the power 2.00. For a streamlined body, drag is proportional to velocity to the power 1.50—a less drastic increase. For the present thalli, the exponent is still lower, 1.14; so drag is more nearly proportional to the first than to the second power of flow speed.

It is customary to consider the manner in which the drag coefficient varies with the Reynolds number instead of how drag varies with speed (see Vogel, 1981; 1984). For a given object in a given medium, the drag coefficient is proportional to drag divided by the square of speed and Reynolds number is proportional to speed itself. Thus the exponents relating values of drag coefficient and Reynolds number (as in equation 9) may be obtained by subtracting 2.00 from those above, giving 0.00, -0.50 , and -0.86 respectively.

The functional significance of such low drag is not self-evident. As mentioned, it is far below the force needed to detach a thallus at the speeds considered here. What about higher speeds? The results of extrapolations beyond $0.71 \text{ m} \cdot \text{s}^{-1}$ depend on the choice of exponent for the relationship between C_d and Re . In the unlikely event that the splendidly low exponent of -0.86 persists at higher speeds, the weakest alga would detach at $54.8 \text{ m} \cdot \text{s}^{-1}$, far higher than the maximum speeds ever recorded for water flows in nature. Assuming a streamlined body with an exponent of -0.5 gives detachment at $19.3 \text{ m} \cdot \text{s}^{-1}$, comparable to the highest speeds in storms on exposed rocky coasts (Vogel, 1981; Denny, 1982). For a bluff body and an exponent of 0.0, probably an unreasonably conservative assumption, detachment would occur at $8.5 \text{ m} \cdot \text{s}^{-1}$, still an heroic velocity. In short, the quality of the streamlining of the *Halosaccion* thallus is far beyond what might be required to resist ordinary hydrodynamic drag.

Two possible explanations of this apparent “overdesign” might be mentioned. (1) The actual drag figures in nature might be higher than those measured here. Thalli frequently bear epiphytes, mainly filamentous algae, which must contribute to their drag. In addition, partially deflated thalli most likely have more drag than fully inflated ones. (2) It is possible that the critical matter is the use of local currents to augment reinflation, as will be discussed below, and that the streamlined shape is, in part, an indirect consequence of design for an appropriate lengthwise pressure distribution.

An additional force tending to detach thalli is the so-called “acceleration reaction,” a force dependent on the acceleration of the fluid relative to a body, the mass of fluid displaced, and a shape-dependent coefficient. For very prolate spheroids, the coefficient is low (Daniel, 1984); and, while water flowing over thalli is constantly changing

speed, the accelerations do not seem to be great. Thus the acceleration reaction is unlikely to be significant in this system.

Emptying and refilling

As anticipated, a set of physical devices, acting in concert, determine the rate at which a thallus empties while it is exposed to air. Two mechanisms promote water loss. *Evaporation* can, as shown here, occur from the thallus wall. It might generate a significant transmural concentration gradient on a sunny, summer day such as that for which DePamphilis (1978) noted that internal water was necessary for survival. *Gravity* will force water out through the pores; it will be most important when a thallus is hanging vertically but will, of course, be largely independent of temperature or illumination. For a thallus 8 cm long with holes mostly about 75% of the way from base to apex, the gravitational pressure will be about 600 Pa.

Another phenomenon, acting at two different points, will oppose water loss. At the pores, *surface tension* will prevent the entry of air through any pore across which the net pressure is inward, that is, where some combination of wall resiliency and other stresses reduce the pressure inside below that outside. Entry of air would, of course, relieve the inward pressure of such mechanical actions and thus permit more rapid egress of water. But the threshold pressure to force air through a pore is greater than any pressure likely to occur naturally. In fact, air-filled thalli are not uncommon during emersion; but they inevitably prove to have been damaged, presumably through the bites of herbivores. Surface tension might also have some effect over the outer surface of a wet thallus in air. Here, though, it is a minor matter, since the radius of curvature is that of the whole thallus and the shape is closer to cylindrical than to spherical. By equation (4b) the inward pressure will only be about 7 Pa.

Refilling, likewise, results from the actions of several physical agencies. Three mechanisms might create an inward movement of water during immersion. *Osmosis* is likely to be minor under most circumstances since the salinity difference across the wall will rarely be very large. However one can imagine occasional cases of occluded pores, substantial rates of evaporation, or gradual increases in salinity through alternating evaporative water loss and bulk sea water replacement in which osmotic refilling might become appreciable. *Wall resilience* appears to be the basic and most consistent mechanism, independent of local flows or the past mechanism of water loss. As determined here, it produces an inward pressure of about 50 Pa, although the variation among individuals is large. Finally there is *flow-induced transmural pressure* resulting from the inverse relationship between speed of flow and pressure along a streamline (Bernoulli's principle). At this point the contribution of the latter is difficult to estimate since it is proportional to the square of flow speed and flow speed is as variable as any parameter of the habitat.

While we believe we have identified the principal mechanisms involved in emptying and refilling, we regard as premature any attempt to draw up a balance sheet reflecting overall pressures, flows, and estimated minimum ratios of immersion to emersion times. Such a balance sheet would, however, permit robust hypotheses concerning the local distribution of the species in the intertidal. Might, for example, more rapid refilling due to faster flows permit survival further above the low water mark?

Characteristics of the pores

Pore morphology will determine the relative importance of different physical processes. Larger pores would allow greater exchange by bulk flow of external sea

water with the water within a thallus when the plant is immersed (and thus more rapid refilling). Small pores will restrict the introduction of air through the pores when the plant is exposed since the pressure difference that an interface can support is inversely related to orifice size (equation 4a). The size and shape of the pores may therefore represent a compromise between keeping air out during emersion and permitting exchange of water during immersion.

Measurements of pressure *versus* flow, of gravity-driven water loss, and of threshold for the entry of air permit calculation of nominal diameters for the pores by equations (3) and (4a) respectively. The results are surprisingly varied. Forcing water through a cannulated thallus leads to an estimate of about 100 μm . The threshold for passage of air implies a diameter of about 300 μm . The rate of water loss for a thallus held vertically in air implies pores of around 20 μm . An ordinarily large pore, according to DePamphilis (1978) is about 100 μm across; our observations agree with his figure. But the pores have a depth greater than their diameter, which will decrease pressure-driven flows; and they are closer to cruciform slits than to circles in cross-section, which will substantially increase the threshold pressure for entry of air as well as decrease pressure-driven flows. In short, pores should have nominal diameters much less than their maximum transverse dimensions, and the figure of 20 μm is probably closer to functional reality than the larger figures. Indeed, by equation (3) a thallus suspended in air with pores of nominal diameter between 100 and 300 μm would deflate with quite unnatural rapidity.

Uncertainties in the measurements, however, are not sufficiently large to account for an order of magnitude overestimate of nominal diameter. A more likely explanation is that the experimental manipulations inadvertently enlarged the pores: even gentle squeezing to expel water, the pressures involved in the cannulations, and those to which the pieces of thallus were subjected functionally enlarged the pores. Only in determining gravitationally driven water loss were the thalli not pressed or squeezed at all. We suggest that in future investigations the absence of visual changes in the pores not be taken as evidence that the pores have not been mechanically altered.

Several phenomena were not encountered. No evidence was found of any mechanical "valving;" curves of pressure *versus* flow were usually linear from the origin in the interesting range of pressures. The resistance of pores to the flow of water was not appreciably different in the two directions. And the threshold for forcing air through pores with water on the other side did not depend on which way the air was forced.

ACKNOWLEDGMENTS

Most of this investigation was carried out in connection with the 1981 and 1983 courses in biomechanics at the Friday Harbor Laboratories of the University of Washington. We thank the personnel of the Laboratories for excellent expediting of material matters and, in particular, the director, A. O. Dennis Willows, for the instigation of the course. C. L. gratefully acknowledges fellowship support from the Laboratories. We also thank Sarah Armstrong, Olaf Ellers, Gayle Hansen, and Michael LaBarbera for advice and assistance.

LITERATURE CITED

- DANIEL, T. L. 1984. Unsteady aspects of aquatic locomotion. *Am. Zool.* 24: 121-134.
DENNY, M. 1982. Forces on intertidal organisms due to breaking ocean waves: design and application of a telemetry system. *Limnol. Oceanogr.* 27: 178-183.

- DEPAMPHILIS, C. 1978. The resistance to damage due to desiccation in the intertidal alga *Halosaccion glandiforme* (Gmelin) Ruprecht. Unpub. MS., Library of Friday Harbor Laboratories, Friday Harbor, WA. Unpaginated.
- GOLDSTEIN, S. 1938. *Modern Developments in Fluid Dynamics*. (Reprint, 1965). Dover Publications, Inc., New York. 702 pp.
- HAPPEL, J., AND H. BRENNER. 1965. *Low Reynolds Number Hydrodynamics*. Prentice-Hall, Englewood Cliffs, NJ. 553 pp.
- MUENSCHER, W. L. C. 1915. Ability of seaweeds to withstand desiccation. *Puget Sound Biol. Sta. Pub.* **1**(4): 19-23.
- ROUSE, H. 1946. *Elementary Mechanics of Fluids*. (Reprint, 1978). Dover, Publications, Inc., New York. 376 pp.
- TUCKER, V. A., AND G. C. PARROTT. 1970. Aerodynamics of gliding flight in a falcon and other birds. *J. Exp. Biol.* **52**: 345-367.
- VOGEL, S. 1981. *Life in Moving Fluids*. Willard Grant Press, Boston. 352 pp.
- VOGEL, S. 1983. How much air passes through a silkworm's antenna? *J. Insect Physiol.* **29**: 597-602.
- VOGEL, S. 1984. Drag and flexibility in sessile organisms. *Am. Zool.* **24**: 37-44.